Creep behavior comparison of CMW1 and palacos R-40 clinical bone cements

C. LIU[1,2*], S. M. GREEN[2], N. D. WATKINS[3], P. J. GREGG[1], A. W. MCCASKIE[1]
[1]*Department of Trauma and Orthopaedic Surgery, University of Newcastle, Newcastle upon Tyne NE2 4HH, UK*
[2]*Centre for Biomedical Engineering, University of Durham, Durham DH1 3LE, UK*
[3]*DePuy CMW, Blackpool FY4 4QQ, UK*
E-mail: Chaozong.Liu@durham.ac.uk

The restrained dynamic creep behaviors of two clinical bone cements, Palacos R-40 and CMW1 have been investigated at room temperature and body temperature. It was found that the two cements demonstrated significantly different creep deformations, with Palacos R-40 bone cement demonstrating higher creep strain than CMW1 bone cement at each loading cycle. For both cements, two stages of creep were identified with a higher creep rate during early cycling followed by a steady-state creep rate. The test temperature had a strong effect on the creep performance of the bone cements with higher creep rate observed at body temperature. The relationship between creep deformation and loading cycles can be expressed by single logarithmic model. The SEM examinations revealed that CMW1 bone cement is more sensitive to defects within the specimen especially to the defects at the edges of the specimen than Palacos R-40 bone cement. However, in the absence of micro-cracks or defects within the inner surface layer, the dynamic loading (at less than 10.6 MPa) is unlikely to produce micro-cracks in the CMW1 bone cement. The different behaviors between the two bone cements may be attributed to differences in chemical compositions and molecular weight distributions.

1. Introduction

The introduction of acrylic bone cement in total hip arthroplasty (THR) has contributed to the success of this surgical procedure [1, 2]. Ironically, the bone cement is also thought of as the weak link in THR, with some studies suggesting that the loosening of cemented THR is related to the cement performance in service [3–6]. A large number of studies reporting the mechanical properties of bone cement and the factors that affect these properties have been reported in the literature [7–11]. However, relatively little attention has been given so far to the time-dependent properties of the bone cement, especially under environmental conditions similar to those experienced *in vivo* [12].

Acrylic bone cement at body temperature behaves in a manner that is neither that of a simple elastic solid, nor that of a true viscous liquid. It behaves as a visco-elastic solid [12] undergoing both elastic and visco-elastic deformation (creep) under load. Verdonschot *et al*. [13] reported that cement creep relaxes cement stresses to create a more favorable stress distribution at the bone cement–stem interface and at the bone–cement interface. Fowler *et al*. [14] postulated that metal–cement interface slip increases the long-term stability of a THR by protecting the cement–bone interface. Harris and colleagues [15] have stated that creep of the cement mantle surrounding a hip prosthesis may be negligible under cyclic physiological loading.

Chwivut *et al*. [16] have demonstrated that different brands of bone cement exhibit different creep behaviors under static loads. Norman [17] investigated the creep characteristics of hand and vacuum mixed acrylic bone cement at elevated stress levels and found measurable creep strains, with higher creep strains for the hand-mixed cement specimens compared to the vacuum-mixed ones. Verdonschot *et al*. [18] tested the creep behavior of acrylic bone cement both under tensile loading and under compressive loading conditions. They found a linear relationship between the logarithmic values of the number of loading cycles and the creep strain. All these reported studies were performed on unconstrained cement specimens, however, *in vivo*, bone cement is restrained between the femoral stem and the cortical bone (cancellous bone). Thus, the strain and stress distribution within the constrained cement mantle may differ from that of the restraint-free condition. Prior to this study, few published works have reported on the creep of bone cement under constrained conditions.

*Author to whom all correspondence should be addressed: Centre for Biomedical Engineering, School of Engineering, University of Durham, South Road, Durham DH1 3LE, UK.

CMW1 (DePuy CMW, England) and Palacos R-40 (Heraeus Kulzer Gmbh, Germany) are two widely used bone cement formulations. Early studies of the creep and stress relaxation behaviors of these two cements showed that CMW1 and Palacos R-40 behaved in a significantly different manner [12]. The analysis of physical and mechanical properties highlighted compositional differences between these cements and that CMW1 exhibited increased bending strength and bending modulus in comparison to Palacos R-40 [19, 20]. This may suggest that these two bone cements could behave differently in service. The objectives of this study were to investigate the dynamic creep behavior of these two acrylic bone cements under constrained conditions, and to correlate the loading cycles with the creep deformations. The results obtained may help to understand the creep behavior of the cement mantle in cemented THR.

2. Materials and experimental

2.1. Bone cements and test specimens

Two commercially available clinical bone cements, CMW1 radiopaque (DePuy CMW, England) and Palacos R-40 (Heraeus Kulzer Gmbh, Germany) were used for the present study. The bone cements were two component systems, formed from an initial mixture of polymer powder and monomer liquid. CMW1 bone cement contained $BaSO_4$, while Palacos R-40 contained ZrO_2 as the radiopaque agent. The compositions and size distributions of the investigated bone cements are reported elsewhere [19].

The test specimens were prepared by hand mixing one package (40 g powder, 20 ml liquid) at room temperature following the manufacturer's preparation procedures. The bone cement creep test specimen used was a hollow cylinder, with an inside diameter of 10 mm, outside diameter of 20 and 25 mm in length. This geometry was chosen to approximate that of the *in vivo* femoral component within cortical bone cavity to allow comparison with cemented prosthesis in the femur. The hollow cylindrical mold cavities were filled once the mixed cement reached dough time. The bone cement was allowed to cure at room temperature in the molds for 1 h, then specimens were removed from the molds and cured in water at 37 °C for a period of 1 month.

The creep test specimen and test jig used in this work is illustrated in Fig. 1. The specimen was restrained between the steel outer jacket and inner stainless steel core. The plunger was designed to allow free vertical

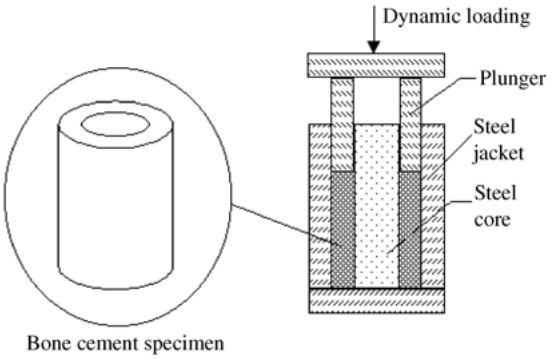

Figure 1 Schematic of creep test specimen and jig.

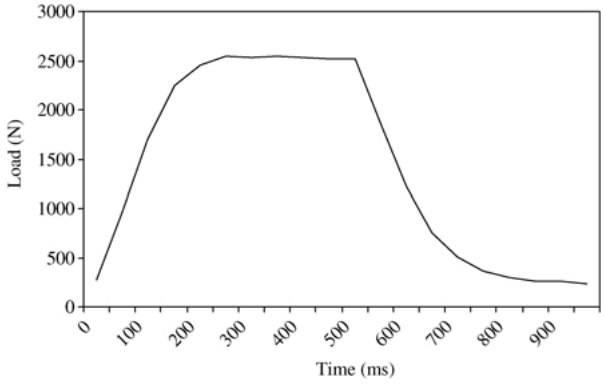

Figure 2 Dynamic loading cycle used for creep test.

movement and was used to apply dynamic compressive loads to the specimen. The creep deformation of the specimens was measured using a micrometer with a resolution of 1 μm.

2.2. Dynamic load profile

The dynamic creep test was conducted on a modified Durham Mk. 2 hip joint simulator. This simulator has six stations [21] and uses a pneumatic actuator and proportional valve for each station. The pneumatic output from these stations generate a square wave loading cycle at a frequency of 1 Hz, as shown in Fig. 2. The compressive load level peaked at 2500 N, which for the sample geometry used generated an equivalent stress of 10.6 MPa, which is the stress level that a well-bonded stem may reach *in vivo*. The dynamic creep tests were conducted at both room temperature and body temperature and were run for six million loading cycles.

3. Results

The creep variations with the loading cycles for the two bone cements at body temperature are shown in Fig. 3(a). This figure illustrates that the bone cement specimens demonstrate creep with respect to time.

It was observed that creep of the specimens for both bone cements (CMW1 and Palacos R-40) increased with the loading cycles. Palacos R-40 bone cement demonstrated higher creep strain than CMW1 bone cement at each loading cycle. Total creep strain after six million cycles reached 0.76% and 0.64% for specimens of Palacos R-40 and CMW1 bone cement respectively.

The creep of the specimens for both bone cements at room temperature (Fig. 3(b)) demonstrated a similar tendency to that at body temperature, i.e., creep strains increased with the loading cycles and Palacos R-40 bone cement creeped more than CMW1 bone cement. Total creep strain reached 0.44% and 0.41% for the specimens of Palacos R-40 and CMW1 bone cements respectively at room temperature. However, in comparison to the creep at body temperature, at room temperature, the two bone cements demonstrated closer similarity in creep behavior.

With reference to Fig. 3(a) and (b), two creep behaviors are evident. A higher creep rate was measured during early cycling, followed by a steady-state creep rate at later cycling. The creep rate during early cycling

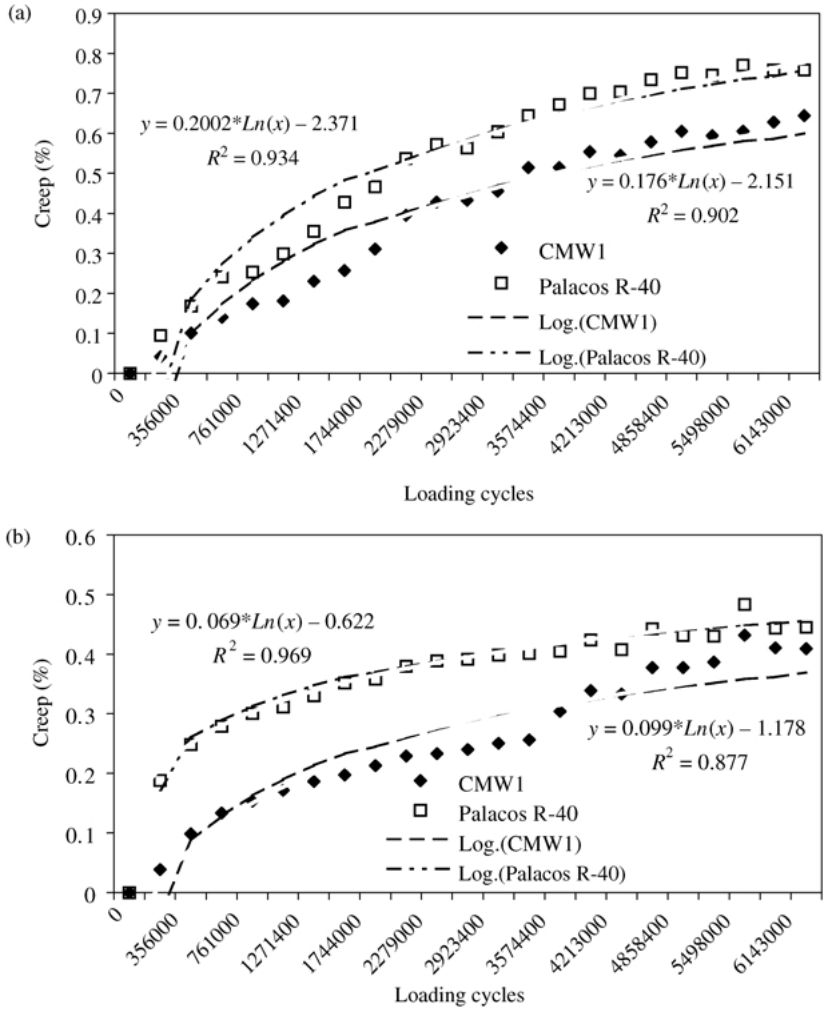

Figure 3 Creep variation with the loading cycles (a) at body temperature and (b) room temperature.

was characterized by rapid increase of creep with loading cycles for both bone cements, at both investigated temperatures. This primary creep stage continued for about one-and-a-half million cycles for the creep test at body temperature, and about one million cycles at room temperature. A creep strain of 0.32%, representing almost half of the total creep deformation for CMW1 bone cement tested at body temperature, was reached only after 1 744 000 loading cycles, beyond which the creep rate tended towards a steady state. The Palacos R-40 bone cement exhibited a higher creep rate compared to CMW1, yielding a creep strain of 0.47% at 1 744 000 cycles, which represents 60% of the total creep for six million loading cycles at body temperature. A similar tendency was also observed for the creep test at room temperature. After the initial creep stage, the creep rate of the specimens tended towards to a steady state.

The regression analysis indicated that relationship between creep strain, ε, and the number of loading cycles, N, can be expressed by the following single logarithmic model:

$$\varepsilon = a \cdot \ln(N) + b \tag{1}$$

where a and b are constants. Application of the above model to the creep data sets, enabled the following relationships between creep strain and loading cycles to be determined.

For the Palacos R-40 and CMW1 specimens tested at body temperature, the following equations were obtained:

$$\varepsilon = 0.2002 \cdot \ln(N) - 2.371 \tag{2}$$

$$\varepsilon = 0.176 \cdot \ln(N) - 2.151 \tag{3}$$

For Palacos R-40 and CMW1 bone cement tested at room temperature is the following equations were obtained:

$$\varepsilon = 0.069 \cdot \ln(N) - 0.622 \tag{4}$$

$$\varepsilon = 0.099 \cdot \ln(N) - 1.178 \tag{5}$$

As a visco-elastic material, the creep behavior of the bone cements is influenced by the test temperature. The effect of test temperature on the creep strains of Palacos R-40 and CMW1 bone cement is shown in Fig. 4(a) and (b) respectively.

It was observed that test temperature had negligible effect on the early creep of the specimens both for Palacos R-40 and CMW1 bone cement.

However, the difference between the creep at body temperature and room temperature widens beyond about one-and-a-half million loading cycles, especially for Palacos R-40 bone cement. An increase of 0.14% for CMW1 and 0.31% for Palacos R-40 was observed after six million loading cycles, upon increasing the test temperature from 20 °C to 37 °C.

Close examination of the Palacos R-40 specimens

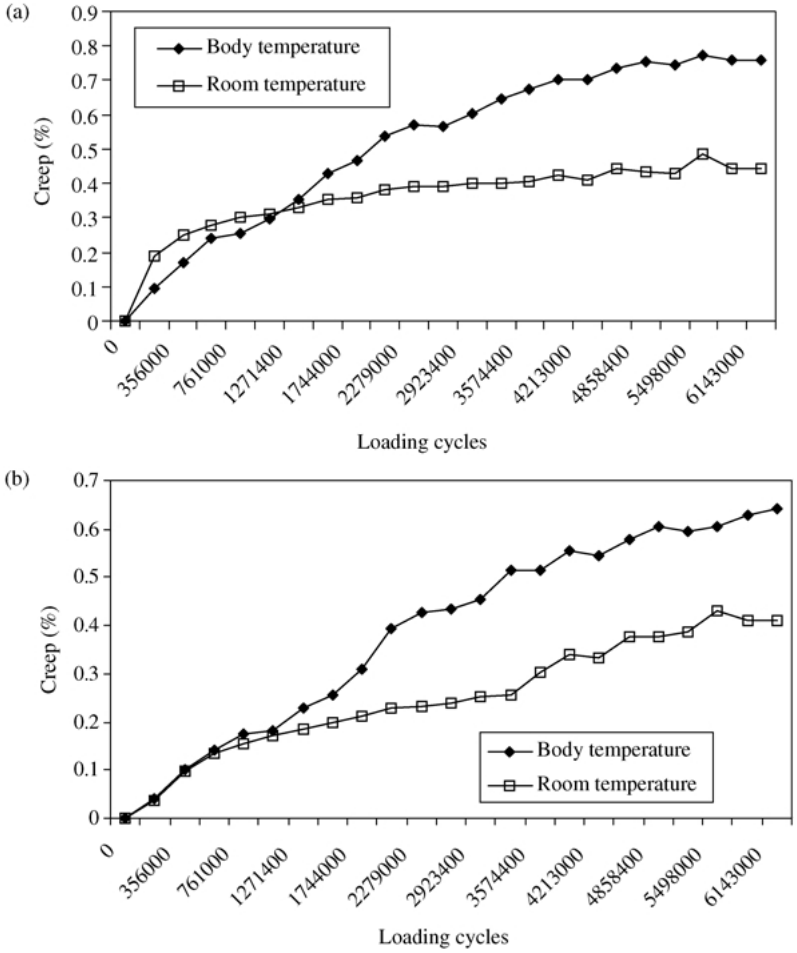

Figure 4 Effect of testing temperature on the creep of the specimens (a) Palacos R-40 and (b) CMW1 bone cement.

revealed that micro-cracks initiated at the inner edge (femoral stem) within the matrix, and propagated about 100 μm deep into the specimen (Fig. 5(a) and (b)). The micro-cracks propagate preferentially through the inter-bead matrix, demonstrating characteristic bead debonding due to matrix failure, as observed elsewhere [19]. In contrast to the Palacos R-40 specimens, no micro-cracks were observed in the CMW creep specimens, the inner edge appeared intact after six million loading cycles, as observed in Fig. 5(c) and (d).

4. Discussions

4.1. Micro-cracks within bone cement

Previous mechanical test results found the bending modulus of CMW1 bone cement (2473 MPa) to be much higher than that of Palacos R-40 (1386 MPa), whereas Palacos R-40 demonstrated much higher impact strength than CMW1 bone cement [19]. Harper and Bonfield [20] studied the static and dynamic tensile performance of a number of bone cements, and reported Palacos R-40 to have considerably higher tensile strength and strain at failure and higher Weibull median fatigue cycles to failure than that of CMW1 bone cement. The fatigue fractured Palacos R-40 cement featured a slow fractured rough surface, while CMW1 featured a fast fractured flat surface, suggesting CMW1 cement to be more brittle. As rigid bone cement (compared to Palacos R-40), CMW1 tends to creep less when subject to dynamic loading. Conversely, the higher creep deformation and high porosity in Palacos R-40 bone cement (Fig. 6) can absorb part of the dynamic impact energy. This phenomenon was again confirmed by the creep observations that Palacos R-40 bone cement creeps more than CMW1 bone cement under the same test environment. CMW1 bone cement is more sensitive to the impacting effects than Palacos R-40 bone cement.

In order to test this hypothesis, the bone cement creep specimens were formed by machining into the cylinder shape from solid cement rather than by casting. SEM examination of these machined cement samples showed that micro-cracks were initiated by the machining process at the inner surface of the CMW1 specimens, and that these cracks propagated with loading cycles deep into the specimen, as shown Fig. 7. Conversely, no obvious micro-cracks were observed on the machined Palacos R-40 specimen sections. The inner machined surface was instead characterized by a localized and narrow bead loosened zone (shown in Fig. 8).

This observation confirms the notch sensitivity of CMW1 bone cements and illustrates the detrimental effect of surface defects, such as micro-cracks. Once the micro-cracks are initiated, they act as the stress concentrators, readily propagating deep into the specimen. However, in the absence of such defects, the dynamic loading at the investigated stress level (less than 10.6 MPa) is unlikely produce micro-cracks in CMW1 bone cement, as observed in Fig. 5(c) and (d). In contrast

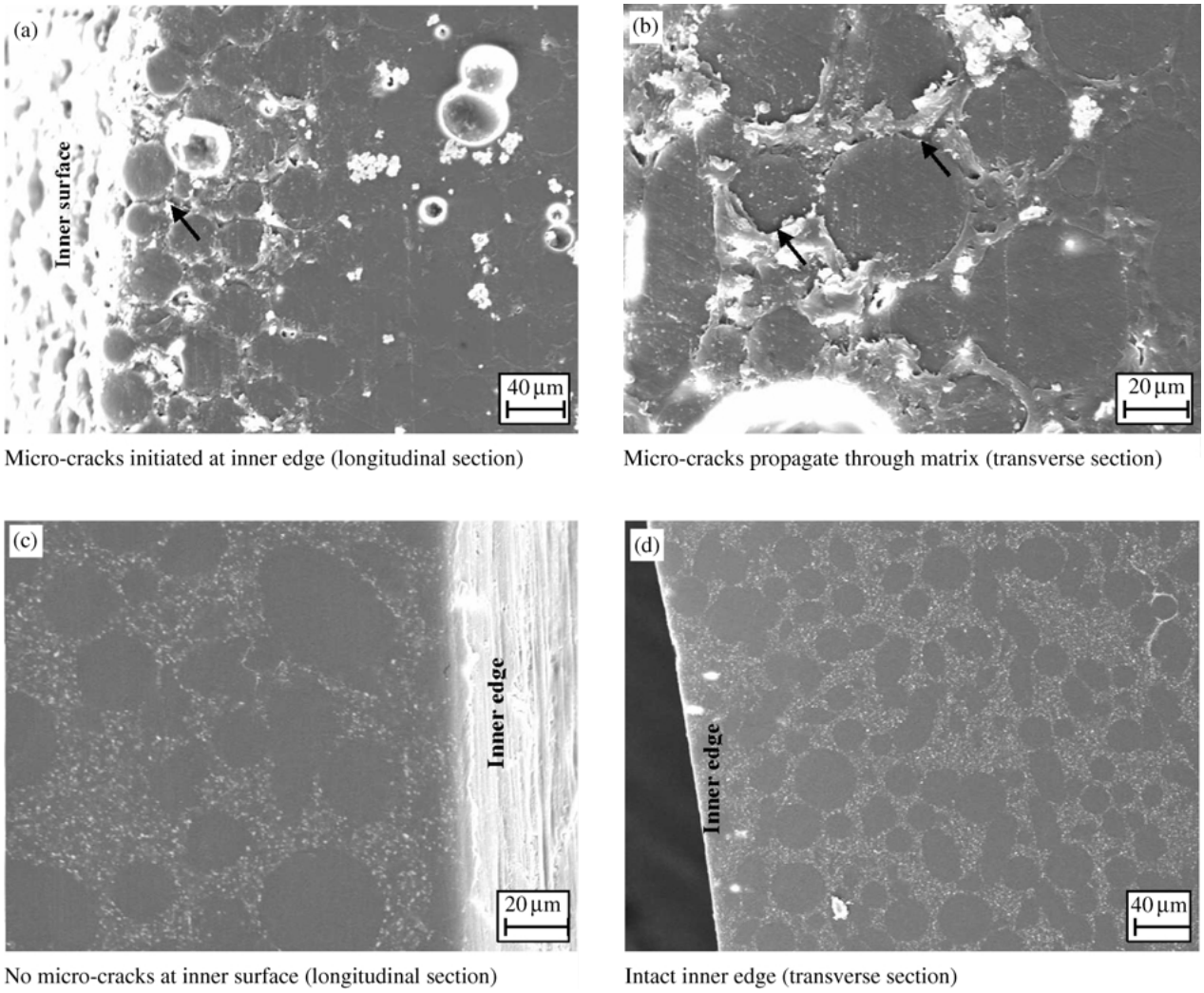

Figure 5 (a) and (b) Micro-cracks initiated at the inner edge and developed into specimen (Palacos R-40 specimen); (c) and (d) no cracks within CMW1 specimens.

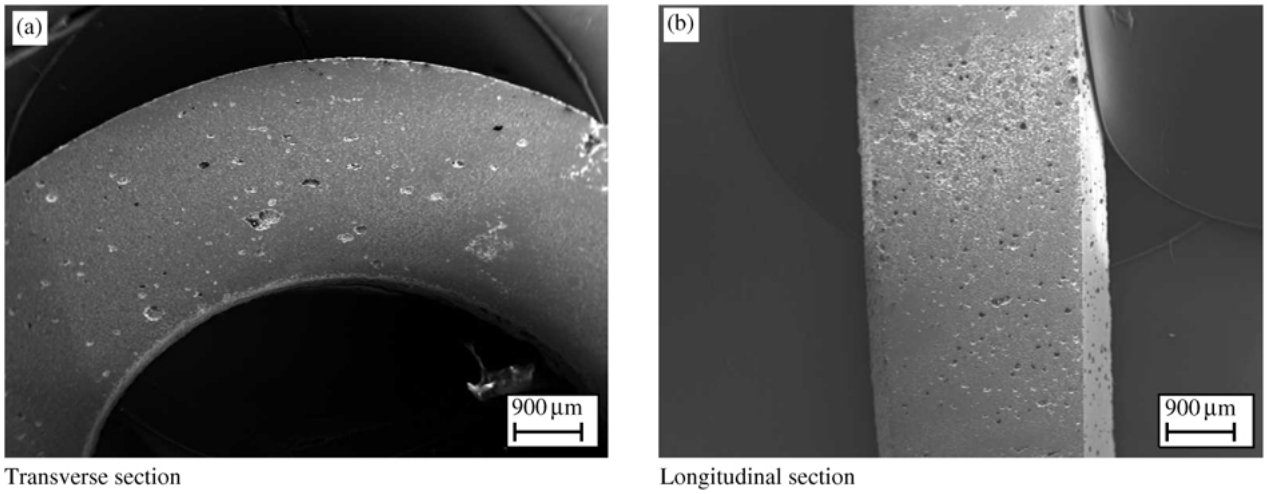

Figure 6 SEM examination revealed high porosity of Palacos R-40 specimens. (a) Transverse section; (b) longitudinal section.

to CMW1 bone cement, Palacos R-40 cement is more ''ductile'' and able to better absorb the machining impact energy. This behavior reduces the notch sensitivity of Palacos R-40 cement in comparison to CMW1, resulting in less damage during machining process.

Based on the above observations, it may be reasonable to suppose that if no pre-existent micro-cracks or defects occurred within the cement mantle surface layer in the bone–bone cement–prosthesis complex, cracks would be unlikely to develop within cement mantle *in vivo* during normal daily physical activity. However, if micro-cracks or defects pre-existed within the stem–cement interfacial zone, the micro-cracks are likely to propagate deep into the cement mantle when it is subjected to normal dynamic loading. This mechanism can explain the mechanical failure of the cement mantle,

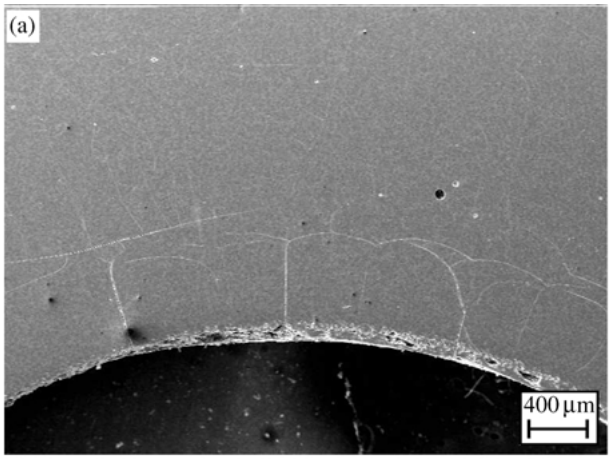

Figure 7 Micro-cracks caused by (a) machining initiated at the inner surface layer and (b) propagate deep into the specimen with the loading cycles (three million cycles) for CMW1 bone cement.

leading to the loosening of the cemented prosthesis in extreme cases.

Several factors should be considered when interpreting the data. The current study was carried out under dry conditions. Acrylic bone cement is a visco-elastic material, and thus creep strains are expected to depend upon environmental conditions. Moisture may have an important effect on the visco-elastic behavior of bone cement, via the reported plasticization effect [22]. Under such conditions, bone cement may behave in a less rigid manner, and it is possible that fewer micro-cracks would have been produced in a more plasticized cement when subject to dynamic loading.

4.2. Factors affecting creep

Creep behavior of hand-mixed bone cements, at several constant stresses levels, has been investigated and demonstrated by Norman *et al*. [16, 17] at room temperature. Their results indicated that creep strain after 24 h remained well below 1%. After 1000 h of a constant applied stress of 12.1 MPa, creep strain did not exceed 1%. They revealed that creep strain substantially increased at higher stress levels and increased non-linearly with increasing applied stress.

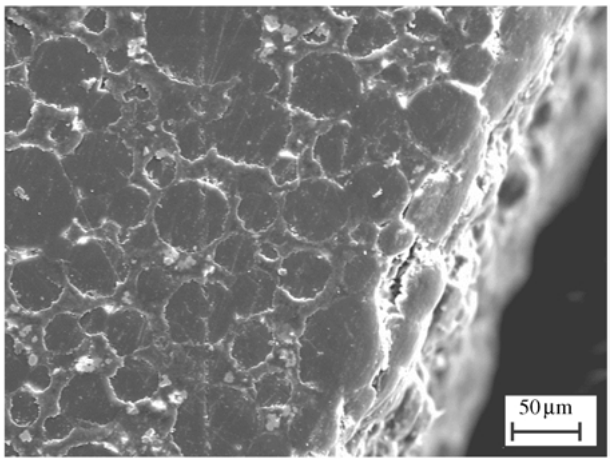

Figure 8 Localized bead loosening on inner surface of Palacos R-40 bone cement specimen following machining.

The creep phenomenon has been described as a stretching and re-aligning of molecular chains of acrylic bone cement. The ambient temperature has a significant effect on this process and high temperature facilitates the re-aligning of the molecular chains, resulting in high creep deformation. Lee *et al*. [12] found in a series of tests designed to emulate the body's environment more closely that creep at 7 days was slower than at 2 days as expected. However, creep at 21 days and 42 days showed a reverse trend, with creep rates increasing. They concluded from their results that cement will creep at *in vivo* stress levels and that it is very sensitive to the ambient temperature and environment. The different cement has different compositions, added by the constrained conditions, may leading to the different creep process.

Chemical compositions and micro-structural properties affect the creep behavior of bone cement. Polymerization of the liquid monomer gives rise to a polymer matrix that surrounds the pre-polymerized PMMA beads. Thus, the performance of the matrix will have a strong influence on the mechanical behavior of the cement. The molecular weight (Mw) of the interstitial matrix polymer for CMW1 bone cement is much higher than the Mw of the pre-polymerized PMMA beads. Conversely, the Mw of the interstitial matrix for Palacos R-40 bone cement is lower than that of the pre-polymerized PMMA beads, as listed in Table I. Generally speaking, the Mw of a polymer influences mechanical properties and physical properties such as hardness and rigidity [23]. The difference in molecular weight between matrix and pre-polymerized beads and the presence of the ceramic radiopaque agent will result in elastic moduli mis-match and the generation of contact stresses at interfacial zone between matrix and beads. Under the action of dynamic loading, such contact stresses together with thermal stresses, could lead to

TABLE I Molecular weight of pre- and post-cured bone cement

Bone cement	Cement powder	Cured cement	Cement matrix
CMW1	208 905	444 308	872 741
Palacos R-40	945 000	757 300	654 463

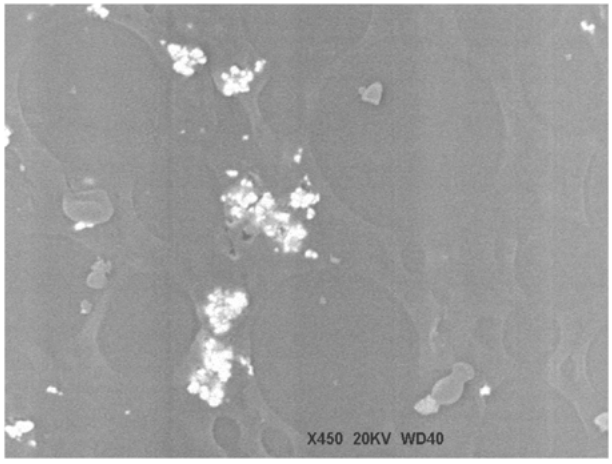

Figure 9 Radiopaque agent agglomerates loosely bonded to Palacos R-40 cement matrix (the radiopaque agent visible as white agglomerates).

beads partially debonding from the matrix, and micro-crack formation and propagation into the specimen.

The debonding of PMMA beads from the matrix formed crevices. The crevices seen in Palacos R-40 bone cement (Fig. 5(a) and (b)), but not in CMW1 bone cement (Fig. 5(c) and (d)), were perhaps attributed to the larger PMMA beads (volume weighted mean size 55 μm for Palacos R-40 and 44 μm for CMW1). As large PMMA beads possess less specific surface area than small beads (such as those found in CMW1 bone cement), this reduces the bead/matrix interfacial zone that transmits load from matrix to bead on dynamic loading. Reduced interfacial zone and contact areas are associated with higher the interfacial stresses. When the interfacial stress exceeds the bonding strength between PMMA beads and matrix, the beads will debond from the matrix, and crevices will be produced, which will act as stress concentration sites. Cracks will propagate from these sites when specimens are subject to dynamic load, such as in dynamic creep testing process.

The main component in Palacos R-40 powder (84.5%) is methyl methacrylate–methylacrylate copolymer [24] with a molecular weight of $945\,000\,g\,mol^{-1}$. When mixed with the liquid component, the copolymer partly dissolves to form the polymethyl methacrylate matrix. CMW1 bone cement powder contains 88.85% (%w/w) of polymethyl methacrylate with a much lower molecular weight of $209\,000\,g\,mol^{-1}$. And such the composition and structure is closer to that of the liquid monomer than the methyl methacrylate–methylacrylate copolymer in Palacos R-40 powder. The higher compatibility may enhance the bonding strength between beads and matrix in CMW1 over Palacos R-40 cement. Owing to the lower molecular weight of CMW1 powder compared to that of Palacos R-40 beads, CMW1 pre-polymerized PMMA beads swelling more and dissolve more. The co-contribution of the higher compatibility and increased swelling and dissolution may be the reason why fewer crevices are found around PMMA beads in CMW1 bone cement, where as crevices were observed in Palacos R-40 bone cement under the same loading conditions.

It is of note that Palacos R-40 bone cement contains a high concentration of radiopacifier ZrO_2 (14.8%). The addition of $BaSO_4$ or ZrO_2 particles to radiopacify the compound is thought to be associated with incomplete particle dispersion during mixing of the monomer and powder component which lead to particle agglomerates. These particle agglomerates can be weakly bonded to the matrix, and the interfacial zone between these particle agglomerates and matrix is a weak link enabling crevices to form, as observed in Fig. 9.

5. Conclusions

This study has shown that Palacos R-40 and CMW1 bone cements demonstrate significantly different creep deformations. Palacos R-40 bone cement demonstrated higher creep strain than CMW1 bone cement at each loading cycle. Creep of the specimens for both bone cements (CMW1 and Palacos R-40) increased with the loading cycles. Two stages, a higher creep rate during early cycles followed by a steady-state creep stage, were identified which are hypothetically governed by two different creep mechanisms for CMW1 and Palacos R-40 bone cement. The test temperature had a strong effect on the creep performance of the bone cements, especially during the later cycling. Bone cements creep more at body temperature than at room temperature. The relationship between the creep deformation and loading cycles can be expressed by a single logarithmic model.

CMW1 bone cement is particularly sensitive to defects within the specimen, especially those at the edges of the specimen. Once micro-cracks are initiated, they act as the stress concentrators, readily propagating deep into the specimen. However, in the absence of such defects, the dynamic loading at the investigated level (less than 10.6 MPa) is unlikely to produce micro-cracks in CMW1 bone cement. In contrast to CMW1 bone cement, Palacos R-40 cement is more ''ductile'' and able to better absorb the machining impact energy. This behavior reduces the notch sensitivity of Palacos R-40 cement in comparison to CMW1, resulting in less damage following machining.

Reference

1. E. EBRAMZADEH, M. MINAARGHI and I. C. CLARKE, ''Loosening of Well Cemented Total Hip Femoral Prosthesis Due to Creep of the Cement'', (ASTM Special Technical Publication, 1985).
2. ORTHOPAEDIC HOSPITAL LOS ANGELES, ''Total Hip Arthroplasty: A Manual for Prospective Patients'' (2000).
3. A. FAULKNER, L. G. KENNEDY, K. BAXTER, J. DONOVAN, M. WILKINSON and G. BEVAN, *Health Tech. Assess.* **2** (1998) 1.
4. R. T. MULLER, I. HEGER and M. OLDENBURY, *Arch. Orthop. Trauma Surg.* **116** (1997) 41.
5. B. M. LWAK, O. K. LIM and Y. Y. KIM, *Intern. Orthop.* **2** (1979) 315.
6. Z. LU and H. MCKELLOP, *J. Biomed. Mat. Res.* **34** (1997) 221.
7. S. SAHA and S. PAL, *ibid.* **18** (1984) 435.
8. B. VAZQUEZ, S. DEB and W. BONFIELD, *J. Mat. Sci.: Mat. Med.* **8** (1997) 455.
9. E. LAUTENS and G. W. MARSHALL, *J. Biomed. Mat. Res.* **10** (1976) 837.
10. G. LEWIS, *ibid.* **40** (1999) 143.
11. J. R. DE WIJN, T. J. SLOFF and F. C. M. DRIESSENS, *Acta. Orthop. Scand.* **46** (1975) 38.
12. A. J. C. LEE, R. D. PERKINS and R. S. M. LING, in ''Implant Bone Interface'', edited by J. Older (Springer-Verlag, London, 1990) p. 85.

13. N. VERDONSCHOT and R. HUISKES, *J. Bone Joint Surg.* **79-B** (1997) 665.
14. J. L. FOWLER, G. A. GIE and R. S. M. LING, *Orthop. Clin. North Am.*, **19** (1988) 477.
15. W. H. HARRIS, *Clin. Orthop. Rel. Res.* **274** (1992) 120.
16. D. J. CHWIRUT, *J. Biomed. Mat. Res.* **18** (1984) 25.
17. T. L. NORMAN, V. KISH and J. D. BLAHA *et al.*, *J. Biomed. Mat. Res.* **29** (1995) 495.
18. N. VERDONSCHOT and R. HUISKES, *J. Appl. Biomat.* **5** (1994) 235.
19. C. Z. LIU, S. M. GREEN, N. D. WATKINS, P. J. GREGG and A. W. MCCASKIE, *Proc. Instn. Mech. Engrs: Part H* **215** (2001) 359.
20. E. J. HARPER, W. BONFIELD *J. Biomed. Mat. Res. (Appl. Biomat.)* **53** (2000) 605.
21. S. L. SMITH, I. C. BURGESS and A. UNSWORTH, *Proc. Instn. Mech. Engrs: Part H* **213** (1999) 469.
22. J. C. ARNOLD and N. P. VENDITTI, *J. Mat. Sci.: Mat. Med.* **12** (2001) 707.
23. S. A. VISSER, R. HERGENROTHER and S. L. COOPER, in ''Biomaterials Science'', edited by B. D. Ratner (Academic Press, San Diego, California, USA, 1996) p. 60.
24. G. DEANE, W. EGE and W. ELSON, in ''Palacos with Gentamicin: A Practical Guide'' (Schering-Plough Ltd., Mildenhall, Suffolk, 1999).

Received 13 December 2001
and accepted 15 May 2002